Journal of Biomolecular NMR, **11:** 221–226, 1998.
KLUWER/ESCOM

Accurate quantitation of water–amide proton exchange rates using the Phase-Modulated CLEAN chemical EXchange (CLEANEX-PM) approach with a Fast-HSQC (FHSQC) detection scheme

Tsang-Lin Hwang[a], Peter C.M. van Zijl[a,b] and Susumu Mori[a,b,*]
Departments of [a]Radiology and [b]Biophysics and Biophysical Chemistry, School of Medicine, Johns Hopkins University, 217 Traylor Building, 720 Rutland Avenue, Baltimore, MD 21205-2195, U.S.A.

Received 13 November 1997; Accepted 13 December 1997

Key words: CLEANEX-PM, hydrogen exchange, NOE, protein, pulsed field gradients, water

Abstract

Measurement of exchange rates between water and NH protons by magnetization transfer methods is often complicated by artifacts, such as intramolecular NOEs, and/or TOCSY transfer from C^{α} protons coincident with the water frequency, or exchange-relayed NOEs from fast exchanging hydroxyl or amine protons. By applying the Phase-Modulated CLEAN chemical EXchange (CLEANEX-PM) spin-locking sequence, 135°(x) 120°(−x) 110°(x) 110°(−x) 120°(x) 135°(−x) during the mixing period, these artifacts can be eliminated, revealing an unambiguous water–NH exchange spectrum. In this paper, the CLEANEX-PM mixing scheme is combined with Fast-HSQC (FHSQC) detection and used to obtain accurate chemical exchange rates from the initial slope analysis for a sample of ^{15}N labeled staphylococcal nuclease. The results are compared to rates obtained using Water EXchange filter (WEX) II-FHSQC, and spin-echo-filtered WEX II-FHSQC measurements, and clearly identify the spurious NOE contributions in the exchange system.

Magnetization transfer techniques have been successfully applied to study the exchange process of protons between solvent water and exchangeable sites in biomolecules (Gemmecker et al., 1993; Grzesiek and Bax, 1993a; Mori et al., 1994; Dalvit and Hommel, 1995; Koide et al., 1995; Birlirakis et al., 1996; Böckmann et al., 1996; Knauf et al., 1996; Wider et al., 1996; Andrec and Prestegard, 1997). The most common way to detect water-macromolecule interactions in these studies is to selectively excite water and observe the magnetization transfer to other sites. However, these studies are often complicated by artifacts due to other magnetization transfer mechanisms such as (i) NOEs from C^{α}Hs which have chemical shifts coincident with water or (ii) exchange-relayed NOEs from rapidly exchanging protons (hydroxyl or amine groups). Although it has been shown that the NOE peaks from C^{α}H protons can be effectively suppressed by using a purge scheme for ^{13}C labeled samples (Gemmecker et al., 1993; Grzesiek and Bax, 1993a) or a spin-echo filter for non-labeled samples (Mori et al., 1996a), ambiguity still remains due to the contribution of exchange-relayed NOEs. For the analysis of this latter contribution, comparison of NOESY (Jeener et al., 1979) and ROESY (Bothner-By et al., 1984; Bax and Davis, 1985) data has been used to identify whether exchange-relayed NOEs exist in the exchange spectrum (Grzesiek and Bax, 1993a). The underlying principle is that NOE peaks have different polarity between these two types of experiments, whereas exchange peaks are of the same sign. However, when the two processes overlap, quantitation of pure exchange rates is not straightforward. An alternative approach to remove exchange-relayed NOE contributions is by using a NOESY-ROESY mixing scheme (Fejzo et al., 1990, 1991; Liepinsh et al., 1992; Norton et al., 1994; Birlirakis et al., 1996; Knauf et al., 1996; Hwang et al., 1997). For macromolecules in the slow-motion limit, the ratio of cross-

*To whom correspondence should be addressed.

relaxation rates for ROE versus NOE is 2 to −1. Proper manipulation of magnetization trajectories to let the spins spend twice as much time along the z-axis than in the xy-plane can, therefore, cancel NOE and ROE contributions (Griesinger et al., 1988). This approach can remove intramolecular NOEs/ROEs and exchange-relayed NOEs/ROEs simultaneously, leaving only pure exchange contributions. Thus, accurate quantitation becomes feasible. Among these tailored mixing sequences, the CLEANEX-PM spin-locking module (Hwang et al., 1997), 135°(x) 120°(−x) 110°(x) 110°(−x) 120°(x) 135°(−x), is more efficient than others (Fejzo et al., 1991; Norton et al., 1994) in suppressing cross-relaxation and TOCSY contributions within the working bandwidth, and is convenient to implement on spectrometers, because it requires only a 180° phase shift of radiofrequency (rf) pulses.

Previously, we have reported a study of rapidly exchanging backbone amide protons in staphylococcal nuclease (SN) measured by a NOESY type magnetization transfer technique (WEX II) (Mori et al., 1997). This study indicated that some residues, such as D77 and T120, have very low pH dependence and possible involvement of exchange-relayed NOEs. In the present paper, we perform a quantitative exchange study using CLEANEX-PM on the same system and compare the results to those from WEX II. To accomplish this, we extended the CLEANEX-PM approach to a two-dimensional version by incorporating Fast-HSQC (FHSQC) spectroscopy (Mori et al., 1995) as the detection scheme to resolve peaks along the ^{15}N indirect dimension. The effective exchange rates are quantitated by using initial slope analysis. For pure exchange residues, we found good agreement between the two methods, validating the use of the newly designed CLEANEX-PM mixing scheme for quantitative purposes. On the other hand, CLEANEX-PM showed apparently lower exchange rates for several residues, which is attributed to the elimination of the NOE contribution. The extent and origin of such NOE contributions will be discussed.

The (CLEANEX-PM)-FHSQC sequence is outlined in Figure 1. After selective water excitation, the CLEANEX-PM spin-locking module is applied during the mixing period, in which chemical exchange between water and NH protons takes place. The rf pulses in CLEANEX-PM continuously move the magnetizations to different angles to accomplish cancellation of ROEs and NOEs. Although complete cancellation within $\pm 0.5\gamma B_1$ working bandwidth cannot be achieved due to off-resonance effects, we have shown that the residual peak intensities are within the experimental noise level (Hwang et al., 1997). When some parts of the protein backbone are more flexible, the slow-motion limit may not hold. In such conditions, negative ROE peaks may contribute slightly more to partially cancel exchange peaks if these peaks are overlapped, resulting in smaller exchange rates. Intermolecular NOEs (Otting et al., 1991) from water to NHs also produce negative peaks. The degree of these contributions can be observed from the CH region of CLEANEX-PM spectra (Hwang et al., 1997), and we found that, at short mixing times, the intensities are negligible compared to measurable exchanging peaks. For quantitative purposes, it should be noted that the mixing time is exactly defined by the CLEANEX-PM modules. At the end of mixing, the FHSQC sequence (Mori et al., 1995) is used as a detection scheme to resolve peaks and to flip water back to the z direction before detection, thereby avoiding water saturation (Grzesiek and Bax, 1993b). A detailed description of the CLEANEX-PM, WEX II and spin-echo-filtered (SEF) WEX II can be found elsewhere (Mori et al., 1996a,b; Hwang et al., 1997).

Experiments were performed at 37 °C on a Varian Unityplus 500 MHz spectrometer equipped with a z-axis gradient and a triple-resonance probe. The sample was 1.5 mM SN (149 residues) at pH 6.8. Hydrogen exchange rates between water and amide protons were measured by WEX II, SEF WEX II, and CLEANEX-PM spectroscopy.

Figure 2 compares the same 2D contour plot obtained using FHSQC (a), and water-selective WEX II-FHSQC (b), SEF WEX II-FHSQC (c), and (CLEANEX-PM)-FHSQC (d) pulse sequences. The FHSQC spectrum serves as a reference. The peak for M98 exchanges very rapidly and is broadened below the contour level for the plot in (a). In Figure 2b, chemical exchange peaks from water, NOE peaks from $C^{\alpha}H$ excited by the selective 180° pulse, and exchange-relayed NOE peaks from rapidly exchanging protons (hydroxyl or amine groups) all occur. By using a 40 ms spin-echo filter, NOE peaks from $C^{\alpha}H$ of residues E10, K24, Y27, M32, D40, A58, I72, E75, F76, Y91, Y93 and D95 indicated by solid arrows in Figure 2b, are eliminated (Mori et al., 1997) as shown in Figure 2c. Using CLEANEX-PM (Figure 2d), not only NOE peaks from $C^{\alpha}Hs$, but also exchange-relayed NOE peaks, such as L14, K70, D77, T120 indicated by open arrows in Figure 2c, are suppressed.

The theory for extracting water–NH exchanging rates is well established (Jeener et al., 1979; Schwartz

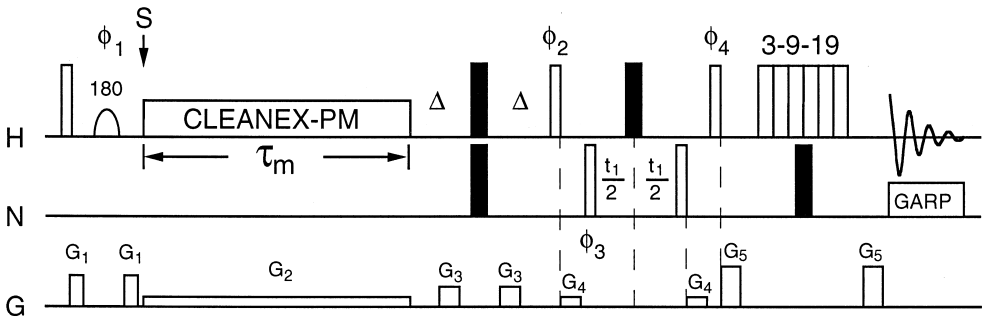

Figure 1. Timing diagram for (CLEANEX-PM)-FHSQC. Open and solid squares represent 90° and 180° pulses, respectively. At 500 MHz, the selective 180° pulse is a 7.5 ms Gaussian. The gradient strengths are $G_1 = 7.0$, $G_2 = 0.1$, $G_3 = 4.4$, $G_4 = 0.2$, and $G_5 = 28.0$ G/cm; the gradient lengths of G_1, G_3, and G_5 are 1 ms, G_4 0.5 ms, and G_2 is applied throughout the mixing period. Phase cycle: ϕ_1 {x,x,y,y}, ϕ_2 {y,y,y,y,−y,−y,−y,−y}, ϕ_3 {x,−x,x,−x}, ϕ_4 {x,x,−x,−x}, and rec.: {x,−x,x,−x,−x,x,−x,x}; the pulse trains in CLEANEX-PM and the 3-9-19 module start from the x direction. Other unspecified pulses are applied in the x direction. The ^{15}N decoupling is accomplished by GARP (Shaka et al., 1985). The interpulse delay in the 3-9-19 pulse module (Sklenář et al., 1993) is 220 μs. The saturation level of water is measured at point S (see text).

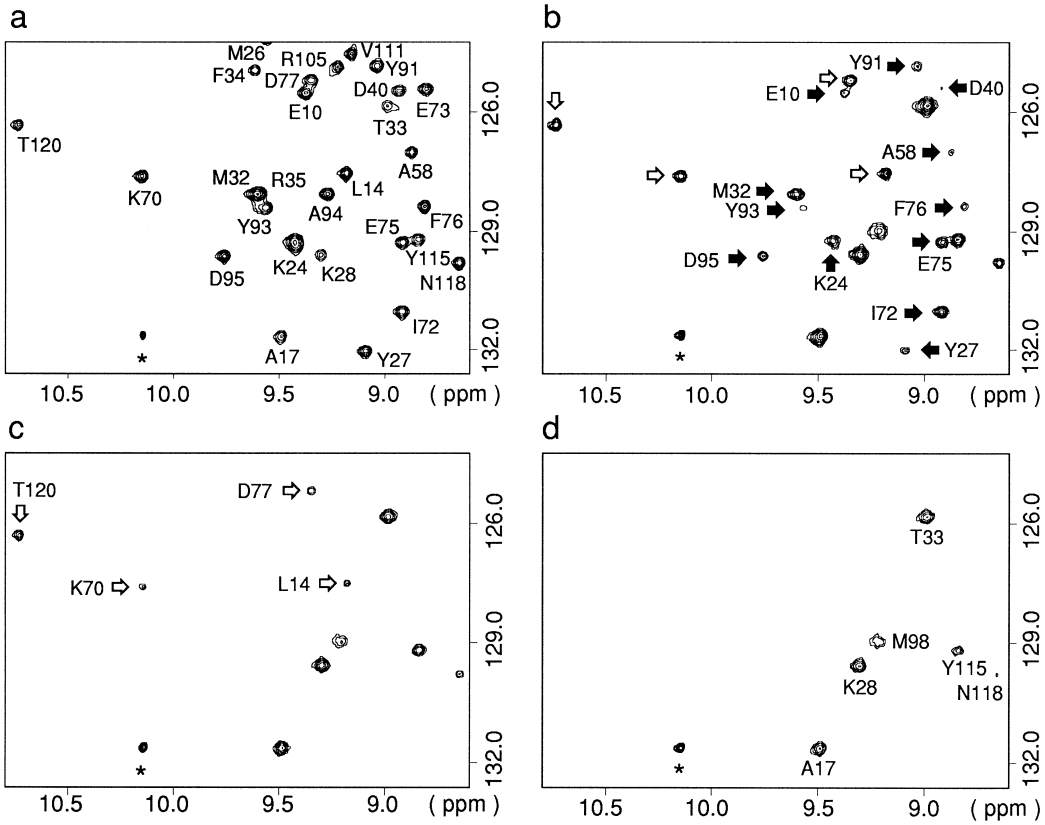

Figure 2. Portion of 2D contour plots for (a) FHSQC, and for water-selective (b) WEX II-FHSQC, (c) spin-echo-filtered WEX II-FHSQC, and (d) (CLEANEX-PM)-FHSQC schemes. In (b) and (c), solid and open arrows indicate intramolecular NOEs and exchange-relayed NOEs, respectively. The mixing time was 100 ms. The spin-locking γB_1 field in CLEANEX-PM was 5.1 kHz. The spin-echo period in WEX II-FHSQC was 40 ms. The spectral widths were 7500 and 2000 Hz for ^{1}H and ^{15}N, respectively. The number of scans was 32 for each increment, with a total of 64 t_1 increments. Contour levels of (b–d) are 1/5 times those in (a). Peaks with asterisks are from a tryptophan side chain.

Table 1. k Values[a] (in s^{-1}) extracted from the initial slope analysis

Residue	WEX-II	CLEANEX-PM
Residues with pure exchange		
G20[b]	3.9±1.0	2.9±0.5
K28	14.4±0.6	14.8±0.3
G29	9.8±0.5	10.5±0.3
G79[c]	6.3±0.5	4.7±0.7
Q80	12.0±0.3	12.8±0.7
R81	23.6±0.4	23.9±1.8
R87[c]	5.7±0.4	4.7±0.7
G96	6.1±1.1	4.5±0.2
M98	51.1±0.5	52.7±1.3
Y115	3.9±0.5	3.5±0.5
Q123	51.3±5.5	55.3±2.5
S141[c]	4.5±0.5	4.8±0.9
D143	28.9±0.7	28.1±1.5
Residues with NOE contributions (> 2 Hz)		
L14	3.3±0.5	[d]
A17[c]	11.3±0.4	7.1±0.4
M32	2.6±0.2	[d]
T33	20.0±0.3	16.1±0.5
K70[c]	3.1±0.5	[d]
I72	5.3±0.5	[d]
E75	2.8±0.3	[d]
D77	2.6±0.2	[d]
A112	2.8±0.3	[d]
T120	3.0±0.5	[d]

[a] Obtained from Equation (1) and divided by 0.85 for CLEANEX-PM and 0.87 for WEX-II data to reflect the water saturation.
[b] NH protons classified as buried and non-hydrogen-bonded in the crystal structure (Mori et al., 1997).
[c] NH protons classified as buried and hydrogen-bonded in the crystal structure.
[d] Exchange rates below the detection limit (∼0.5 Hz).

and Cutnell, 1983; Dobson et al., 1986; Mori et al., 1996b), and the following equation is used to fit k and $R_{1A,app} + k$:

$$\frac{V}{V_0} = \frac{k}{(R_{1A,app} + k - R_{1B,app})} \times \{\exp(-R_{1B,app}\tau_m) - \exp[-(R_{1A,app} + k)\tau_m]\} \quad (1)$$

where k is the normalized rate constant related to the pseudo-first-order forward rate constant $k_{AB}(NH \rightarrow H_2O) = X_B k$; X_B, the mole fraction of water, is ≈ 1. For WEX II experiments, $R_{1A,app}$ is the true $R_{1A} = 1/T_{1A}$, while, in the CLEANEX-PM experiments, the value of $R_{1A,app}$ depends on the trajectory of magnetization, and, thus, is a combination of longitudinal and transverse relaxation rates; τ_m is the mixing time; the peak volume V was obtained from the WEX II-FHSQC, SEF WEX II-FHSQC, and (CLEANEX-PM)-FHSQC spectra at mixing times of 5, 10, 15 and 20 ms; the reference peak volumes, V_0, were measured from the FHSQC spectrum. $R_{1B,app}$ values were measured by separate experiments, in which the dependence of the water signal on mixing times was observed using the 1D WEX and 1D CLEANEX-PM sequences without water suppression. $R_{1B,app}$ values of 0.3 and 0.6 s^{-1} were found from the fitting of WEX II and CLEANEX-PM results, respectively. At very short mixing time, k in Equation (1) reflects the initial slope. It should be noted that the data taken up to $\tau_m = 20$ ms do not provide sufficient constraint for accurate fitting of $R_{1A,app}$. During the measurement of V and V_0, an interscan delay of 2 s was used. For accurate quantitation, the degree of water saturation in each experiment was also determined as follows. To attain the equilibrium condition for water in experiments with predelay times of 2 s and 30 s, 8 dummy scans were used to go through the entire sequence with 5 ms mixing. Then the area of the water peak (Mao et al., 1994) before mixing (point S in Figure 1) was measured. By taking the ratio of the water areas at 2 s and 30 s predelay, it was found that the water intensity remains at 87% for WEX II-FHSQC, and 85% for (CLEANEX-PM)-FHSQC. Assuming that the saturation of water leads to the decrease in intensity for pure exchange peaks in the same proportion, the exchange rate obtained from Equation (1) can be corrected by simply dividing k by 0.87 for WEX II and 0.85 for CLEANEX-PM experiments. When performing the same experiment for the SEF WEX II sequence, the water intensity decreased to 60%, mainly due to water T_2 relaxation during the 40 ms TE.

Figure 3 shows initial slope analysis applied to some representative peaks with different features. Figure 3a shows examples of pure chemical exchange peaks (NHs of K28 and G29). The difference in peak volumes at longer mixing time between WEX II and CLEANEX-PM is due to different relaxation mechanisms during the mixing period (Jeener et al., 1979; Hwang and Shaka, 1993). It is apparent that data points at short mixing times are important for extracting correct chemical exchange rates. SEF WEX II shows lower intensity due to a higher level of water saturation. The method to obtain exchange rates

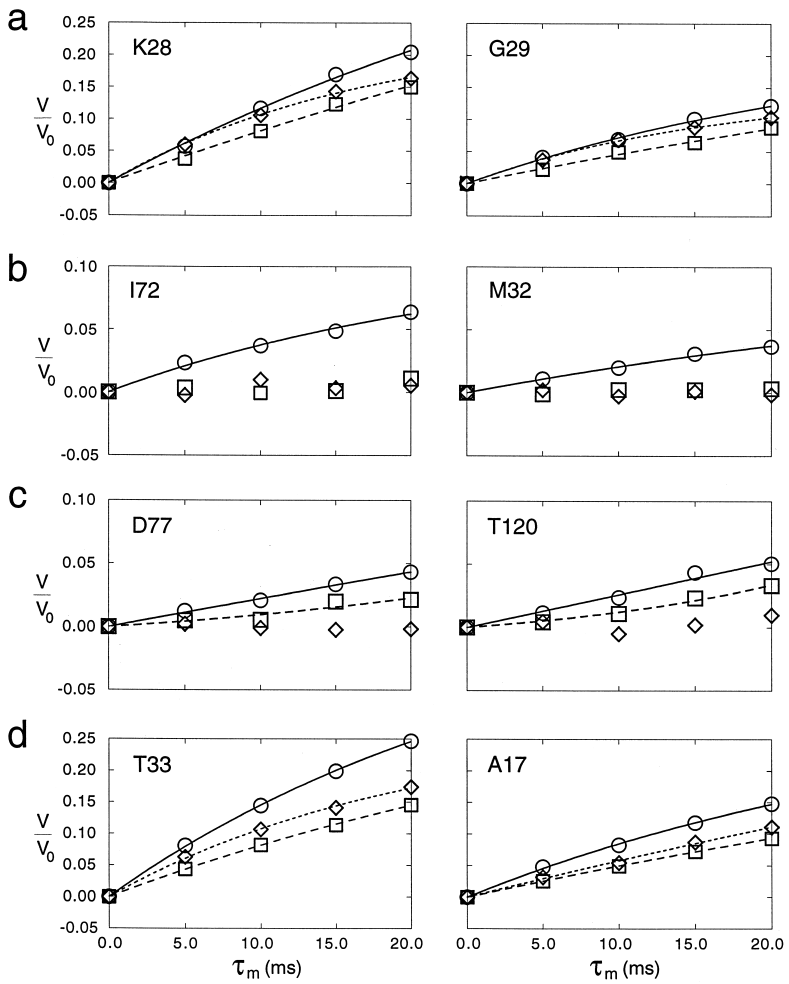

Figure 3. Examples of initial slope analysis applied to peaks with different features shown in Figure 2: (○) for WEX II-FHSQC; (□) for spin-echo-filtered WEX II-FHSQC; and (◇) for (CLEANEX-PM)-FHSQC. These points were plotted without the correction for water saturation factors. (a) Pure chemical exchange at NHs of K28 and G29; (b) pure intramolecular NOEs at NHs of I72 and M32; (c) pure exchange-relayed NOEs at NH of T120; and (d) simultaneous occurrence of chemical exchange and NOEs at NHs of T33 and A17. The NOE at D77 NH is possibly from a bound water molecule, which is suppressed in the CLEANEX-PM experiment shown in (c). Except for the mixing times, the experimental conditions were the same as indicated in the legend of Figure 2. The vertical scale in (b, c) is expanded to twice that in (a, d).

for SEF WEX II data through the water saturation factor has been described in detail elsewhere (Mori et al., 1996a). Figure 3b shows examples of pure intramolecular NOEs (NHs of I72 and M32) which are eliminated in both SEF WEX-II and CLEANEX-PM experiments. Results in Figure 3c are examples of pure exchanged-relayed NOEs in which intensities can only be removed by CLEANEX-PM (NHs of D77 and T120). Figure 3d shows examples of peaks with mixed contributions from chemical exchange and NOEs (NHs of A17 and T33), where chemical exchange rates can be obtained from the CLEANEX-PM data, and the rate difference between the CLEANEX-PM and WEX II data represents the NOE contribution.

Table 1 lists the results from the WEX II and CLEANEX-PM experiments for all measurable residues. Good agreement is found between the exchange rates, suggesting the validity of the CLEANEX-PM data. However, discrepancies between the two were also observed in residues L14, A17, M32, T33, K70, I72, E75, D77, A112, and T120, where rate differences are larger than 2 Hz. Data from SEF WEX II and CLEANEX-PM suggests

that the differences in M32, I72, E75, and A112 are due to NOE contributions from $C^{\alpha}H$; where both data sets show no signal buildup (e.g. Figure 3b). On the other hand, L14, K70, D77, and T120 have additional exchange-relayed NOEs, and only CLEANEX-PM suppresses the signal completely (e.g. Figure 3c). In a previous study exchange rates of amide protons of D77 and T120 were measured at various pH, which revealed poor pH sensitivity. From this study, it is confirmed that these two peaks originate purely from NOE. A17 and T33 are the cases where both chemical exchange and NOE contribute. The measured k values are 11.3, 9.1, and 7.1 Hz for A17 and 20.0, 16.2, and 16.1 Hz for T33 when using WEX II, SEF WEX II, and CLEANEX-PM experiments, respectively. Therefore, for A17, exchanged-relayed NOE and $C^{\alpha}H$ NOE contributions are about 2.0 and 2.2 Hz, respectively. For T33, the difference between WEX II and CLEANEX-PM is due to $C^{\alpha}H$ NOE, because SEF WEX II and CLEANEX-PM give the same k values within experimental error. The 3D crystal structure of SN (Hynes and Fox, 1991) suggests that the source of the exchange-relayed NOEs of L14 and T120 are side chain OHs of T13 and T120, respectively. The origin of exchange-relayed NOEs for A17 and K70 is possibly from side chain amine groups of K16 and K71/K72, respectively. On the other hand, the X-ray study shows no proximal OH or amine group near D77, except a bound water molecule (Hynes and Fox, 1991). This may indicate that the water molecule binds to protein long enough to become the source of a positive NOE peak. The CLEANEX-PM data in Table 1 was verified by using a different γB_1 field at 6.9 kHz, proving the robustness of this approach.

In conclusion, the 2D (CLEANEX-PM)-FHSQC sequence is introduced and applied to the study of solute-solvent proton exchange for SN. The results indicate that accurate quantitation of exchange rates can be achieved, eliminating the ambiguity caused by NOE contributions.

Acknowledgements

The authors thank Dr. David Shortle for providing the sample. This research was supported by NIH grant RR11115 (P.v.Z.).

References

Andrec, M. and Prestegard, J.H. (1997) *J. Biomol. NMR*, **9**, 136–150.
Bax, A. and Davis, D.G. (1985) *J. Magn. Reson.*, **63**, 207–213.
Birlirakis, N., Cerdan, R. and Guittet, E. (1996) *J. Biomol. NMR*, **8**, 487–491.
Böckmann, A., Penin, F. and Guittet, E. (1996) *FEBS Lett.*, **383**, 191–195.
Bothner-By, A.A., Stephens, R.L., Lee, J.-M., Warren, C.D. and Jeanloz, R.W. (1984) *J. Am. Chem. Soc.*, **106**, 811–813.
Dalvit, C. and Hommel, U. (1995) *J. Biomol. NMR*, **5**, 306–310.
Dobson, C.M., Lian, L.-Y., Redfield, C. and Topping, K.D. (1986) *J. Magn. Reson.*, **69**, 201–209.
Fejzo, J., Westler, W.M., Macura, S. and Markley, J.L. (1990) *J. Am. Chem. Soc.*, **112**, 2574–2577.
Fejzo, J., Westler, W.M., Macura, S. and Markley, J.L. (1991) *J. Magn. Reson.*, **92**, 20–29.
Gemmecker, G., Jahnke, W. and Kessler, H. (1993) *J. Am. Chem. Soc.*, **115**, 11620–11621.
Griesinger, C., Otting, G., Wüthrich, K. and Ernst, R.R. (1988) *J. Am. Chem. Soc.*, **110**, 7870–7872.
Grzesiek, S. and Bax, A. (1993a) *J. Biomol. NMR*, **3**, 627–638.
Grzesiek, S. and Bax, A. (1993b) *J. Am. Chem. Soc.*, **115**, 12593–12594.
Hwang, T.-L. and Shaka, A.J. (1993) *J. Magn. Reson.*, **B102**, 155–165.
Hwang, T.-L., Mori, S., Shaka, A.J. and van Zijl, P.C.M. (1997) *J. Am. Chem. Soc.*, **119**, 6203–6204.
Hynes, T.R. and Fox, R.O. (1991) *Proteins Struct. Funct. Genet.*, **10**, 92–105.
Jeener, J., Meier, B.H., Bachmann, P. and Ernst, R.R. (1979) *J. Chem. Phys.*, **71**, 4546–4553.
Knauf, M.A., Löhr, F., Blümel, M., Mayhew, S.G. and Rüterjans, H. (1996) *Eur. J. Biochem.*, **238**, 423–434.
Koide, S., Jahnke, W. and Wright, P.E. (1995) *J. Biomol. NMR*, **6**, 306–312.
Liepinsh, E., Otting, G. and Wüthrich, K. (1992) *J. Biomol. NMR*, **2**, 447–465.
Mao, X., Guo, J. and Ye, C. (1994) *Chem. Phys. Lett.*, **222**, 417–421.
Mori, S., Johnson, M.O., Berg, J.M. and van Zijl, P.C.M. (1994) *J. Am. Chem. Soc.*, **116**, 11982–11984.
Mori, S., Abeygunawardana, C., Johnson, M.O. and van Zijl, P.C.M. (1995) *J. Magn. Reson.*, **B108**, 94–98.
Mori, S., Berg, J.M. and van Zijl, P.C.M. (1996a) *J. Biomol. NMR*, **7**, 77–82.
Mori, S., Abeygunawardana, C., van Zijl, P.C.M. and Berg, J.M. (1996b) *J. Magn. Reson.*, **B110**, 96–101.
Mori, S., Abeygunawardana, C., Berg, J.M. and van Zijl, P.C.M. (1997) *J. Am. Chem. Soc.*, **119**, 6844–6852.
Norton, A., Galambos, D., Hwang, T.-L., Stimson, M. and Shaka, A.J. (1994) *J. Magn. Reson.*, **A108**, 51–61.
Otting, G., Liepinsh, E. and Wüthrich, K. (1991) *Science*, **254**, 974–980.
Schwartz, A.L. and Cutnell, J.D. (1983) *J. Magn. Reson.*, **53**, 398–411.
Shaka, A.J., Barker, P.B. and Freeman, R. (1985) *J. Magn. Reson.*, **64**, 547–552.
Sklenář, V., Piotto, M., Leppik, R. and Saudek, V. (1993) *J. Magn. Reson.*, **A102**, 241–245.
Wider, G., Riek, R. and Wüthrich, K. (1996) *J. Am. Chem. Soc.*, **118**, 11629–11634.